# Experimental study of the production of vortex rings using a variable diameter orifice

J. J. Allen[a)]
*Department of Mechanical and Aerospace Engineering, Princeton University, Princeton, New Jersey 08544*

T. Naitoh[b)]
*Department of Engineering Physics, Electronics and Mechanics, Nagoya Institute of Technology, Gokiso, Showa-ku, Nagoya 466-8555, Japan*

(Received 21 December 2004; accepted 10 March 2005; published online 13 May 2005)

A method for producing a vortex ring with an apparatus that utilizes a time varying aperture that closes during ring production is shown to have the capability for the production of rings of low nondimensional energy similar to a Hill's spherical vortex. This represents a difference of more than 50%, in terms of the nondimensional energy, of those which have been produced with fixed diameter generators. Experiments show that modulation of the rate at which the vortex ring generator produces kinetic energy, circulation, and impulse is the critical factor in determining what type of ring is formed. © *2005 American Institute of Physics*. [DOI: 10.1063/1.1921949]

Experimentally, vortex rings are typically generated by the ejection of a slug of fluid from a cylinder by a moving piston. It has been noted that the nature of the cylinder exit, a tube,[1,2] or an orifice[3] can have subtle effects on the ring properties and evolution. As all of the vorticity in a ring is produced at the walls of the ring generators, different rings are a function of different rates of generation of primary and secondary vorticity. Variations in the final steady state ring are dependent on different temporal and spatial velocity histories at the tube exit during ring formation.[2,4] Gharib *et al.*[5] examined the transition of an impulsively started jet from a single vortex ring to a leading ring with a trailing jet instability. They identified "a universal time scale for vortex ring generation," and found that the maximum nondimensional energy attainable by the lead vortex ring was a function of the piston stroke-to-diameter ratio $L/D$. For a fixed diameter tube, $L/D$ was found to lie in the range 3.6–4.5. In an effort to describe the dynamics of various types of vortex rings use has been made[6] of the Norbury[7] family of vortex rings. The vorticity distribution within the core of Norbury's rings was specified as being proportional to the distance from the axis of symmetry. Norbury[7] computed the boundary of the core, $\delta A$, in terms of a characteristic ring parameter $\alpha$ defined as $\delta A = \pi L_n^2 \alpha^2$, where $L_n$ is the mean core radius. The parameter $\alpha$ varied from 0 to $\sqrt{2}$. This represents the limit between the thin cored vortex solution of Fraenkel[8] and the spherical vortex of Hill.[9] Norbury[7] also calculated the circulation $\Gamma$, impulse $I$, and kinetic energy $E$ for each member of the solution set. The ring invariants, $\Gamma, I$, and $E$, can be reorganized to form two nondimensional parameters, the nondimensional energy $\tilde{E} = E/(\Gamma^{3/2} I^{1/2})$ and the nondimensional circulation $\tilde{\Gamma} = \Gamma/(I^{1/2} U_t^{2/3})$, where $U_t$ is the translational speed of the ring. The ring of the Norbury family that has the lowest nondimensional energy corresponds to a Hill's spherical vortex. Although the distribution of vorticity in experimental rings is typically Gaussian, the Norbury rings provide a framework to consider the experimental trend of ring invariants. The expressions for the energy, impulse, and circulation that are produced by the flow across the nozzle exit with a time varying aperture, with the assumption that the flow is spatially uniform across the exit, give $E_{\text{slug}}(t)/\rho = \pi/8 \int_0^{t_{\text{on}}} U_{\text{exit}}^3(t) D_{\text{ap}}^2(t) dt$, $I_{\text{slug}}(t)/\rho = \pi/4 \int_0^{t_{\text{on}}} U_{\text{exit}}^2(t) D_{\text{ap}}^2(t) dt$, and $\Gamma_{\text{slug}}(t) = 1/2 \int_0^{t_{\text{on}}} U_{\text{exit}}^2(t) dt$. $D_{\text{ap}}(t)$ is the time varying aperture diameter, $t_{\text{on}}$ is the time period that the piston is in motion, and $U_{\text{exit}}(t)$ is the estimated mean speed of the jet from nozzle. This model of the exit flow is often termed the "slug model." By assuming that all the slug invariants were absorbed into the ring Mohseni and Gharib[6] were able to calculate an associated nondimensional energy and hence from the Norbury[7] data they were then able to make an estimate of the associated Norbury parameter $\alpha$ and associated ring speed $W_{\text{Norbury}}$. Some form of closure was still required for pinch-off. It has been established that the behavior of vortex rings obeys Hamiltonian dynamics with $dq/dt = \partial E/\partial I$ where $q$ is the center of the ring.[10] From the slug model Mohseni and Gharib[6] were able to calculate $\partial E_{\text{slug}}/\partial I_{\text{slug}}$ at the tube exit and suggested that when $\partial E_{\text{slug}}/\partial I_{\text{slug}} < W_{\text{Norbury}}$ the ring escapes from the jet. This Letter describes experiments using an apparatus that allows the modulation of the piston speed and the aperture diameter during vortex ring production. The experiments were conducted in a $40 \times 50 \times 100$ cm$^3$ tank.[11] The vortex ring generator consisted of a 5.0 cm diameter piston that moved through a tube. In order to investigate the effect of a time varying aperture, a stainless steel adjustable iris diaphragm was mounted at the tubes exit into the tank. The maximum aperture diameter for the current experiments was chosen as

[a)]Present address: Department of Mechanical Engineering, New Mexico State University, Las Cruces, NM 88003.
[b)]Experiments performed while on sabbatical leave at Princeton University, 2001–2002.

 

TABLE I. Piston velocity and aperture diameter functions.

| | $U_{\text{piston}}$ (cm/s) $=\gamma+\kappa t$ (s) | | $D_{ap}$ (cm) $=\eta+\varphi t$ (s) | | |
|---|---|---|---|---|---|
| | $\gamma$ | $\kappa$ | $\eta$ | $\varphi$ | $\sqrt{t_{\text{on}}/t_1}$ |
| *A* | 4.0 | 0 | 4.0 | 0 | 2.0 |
| *B* | 4.0 | 0 | 4.0 | 0 | 4.0 |
| *C* | 0.25 | 0.38 | 4.0 | 0 | 5.3 |
| *D* | 0.29 | 1.35 | 2.8 | 0.41 | 2.5 |
| *E* | 1.4 | 0 | 4.0 | −0.31 | 3.4 |

4.0 cm. As such the opening is an orifice type rather than a tube exit. Tank water temperature was 22 °C. Particle image velocimetry (PIV) and particle tracking velocimetry (PTV) were used to produce quantitative information about the rings. A Reynolds number definition for the vortex ring is $\text{Re}_D=U_tD_{\text{ring}}/V$, where $U_t$ is translation speed of the ring and $D_{\text{ring}}$ is the ring diameter. A Reynolds number based on the strength (circulation) of the ring is expressed as $\text{Re}_\Gamma=\Gamma/v$. Dynamical properties of the ring that are evaluated from the velocity field data are the impulse per unit mass $I/\rho$, the kinetic energy per unit mass $E/\rho$, and the circulation $\Gamma$. In terms of axisymmetric integrals of the vorticity $\omega(r,x)$ and stream function $\psi(r,x)$ these quantities are expressed as $E/\rho=\pi\int_{-\infty}^{\infty}\int_0^{\infty}\omega\psi dx\,dr, I/\rho=\pi\int_{-\infty}^{\infty}\int_0^{\infty}\omega r^2dx\,dr$, and $\Gamma=\int_{-\infty}^{\infty}\int_0^{\infty}\omega dx\,dr$. The vorticity field was calculated from the velocity field using a global spline technique[12] and the stream function was evaluated by using the vorticity and velocity fields and inverting the Poisson equation.[13] The ring speed, the diameter, and the nondimensional core radius $\alpha$ were also evaluated from the vorticity field data. Selection of the isocontour of vorticity for the calculation of the nondimensional core radius was based on the minimum resolvable vorticity contour, which in these experiments was of the order of 5% of the maximum vorticity level. The ring invariants were then combined to form the parameters $\tilde{E}$ and $\tilde{\Gamma}$. We focused on four different types of generating conditions: (i) Constant piston velocity, fixed orifice diameter to investigate whether a significant difference in the formation number exists between using a tube or orifice. (ii) Constant acceleration of the piston while keeping the orifice diameter fixed. (iii) Accelerating the piston while opening the aperture, as suggested by Mohseni *et al.*[14] (iv) Closing the aperture while moving the piston with constant velocity in an attempt to feed the invariants to the ring via a jet of increasing speed and reducing diameter.

As the aim of the experiments was to produce a ring of low nondimensional energy, it was assumed that for each generation condition, the minimum nondimensional energy was reached when the primary ring pinched-off from the trailing jet. The approximate limiting time was assumed to have been reached when flow visualization experiments revealed coherent vortical structures trailing the main ring. Once this time was determined, detailed PIV/PTV experiments were undertaken. A physical time scale for this experiment can be related to the impulse per unit mass and circulation from the slug model[15] is defined as $t_I=\pi I_{\text{slug}}/(\Gamma_{\text{slug}}^2\rho)$.

TABLE II. Experimental results for ring properties.

| | $\text{Re}_D$ | $\text{Re}_\Gamma$ | $\tilde{E}\pm0.04$ | $\tilde{\Gamma}\pm0.25$ | $\alpha\pm0.07$ | $U_t$ (mm/s) |
|---|---|---|---|---|---|---|
| *A* | 2100 | 5150 | 0.30 | 2.0 | 0.65 | 34 |
| *B* | 2750 | 6400 | 0.29 | 1.7 | 0.80 | 40 |
| *C* | 1050 | 5050 | 0.18 | 2.5 | 0.90 | 22 |
| *D* | 1550 | 3950 | 0.26 | 2.0 | 0.70 | 32.5 |
| *E* | 1850 | 6000 | 0.19 | 2.2 | 0.94 | 41 |

This formulation by definition incorporates the effect of the varying aperture diameter. In the case of a constant diameter orifice one recovers $\sqrt{t_{\text{on}}/t_I}=L/D$ from the work of Gharib *et al.*[5] Details of the piston velocity and aperture diameter programs for the cases investigated in detail are listed in Table I. Results for the experimentally measured values of the Reynolds numbers, nondimensional energy and circulation,

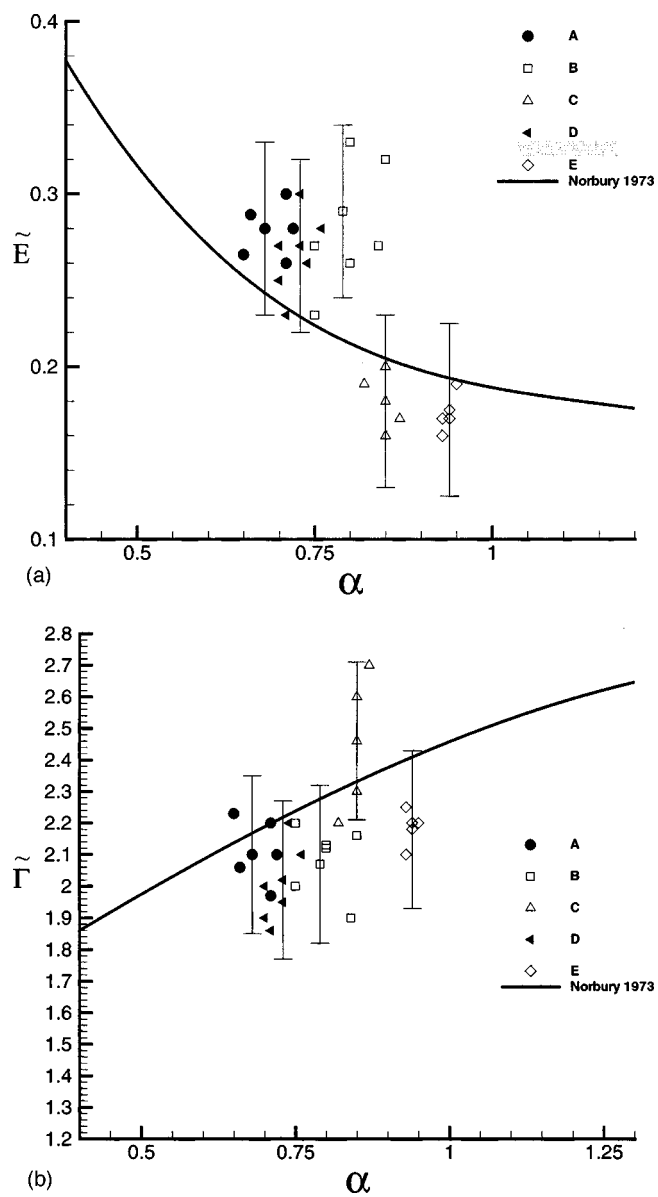


FIG. 1. Results for nondimensional (a) energy and (b) circulation for the range of piston aperture velocity characteristics.

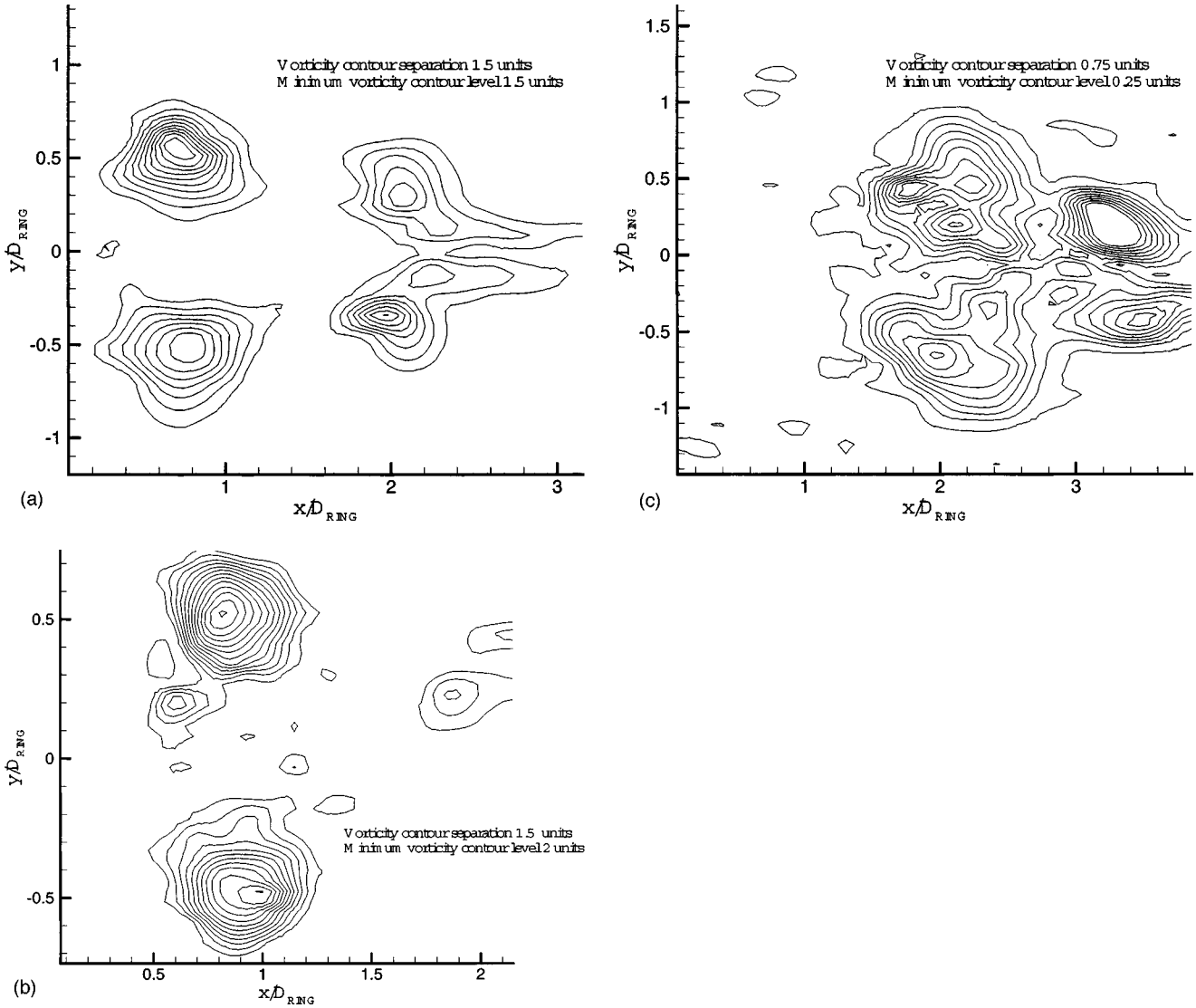


FIG. 2. Plots of normalized vorticity, $\omega^* = \omega D_{\text{ring}}/U_l$, for rings produced with piston/aperture characteristic (a) $B$ at $\sqrt{t/t_I}=5.5$, (b) $D$ at $\sqrt{t/t_I}=4.0$, and (c) $E$ at $\sqrt{t/t_I}=4.5$.

Norbury parameter and speed are listed in Table II. Figure 1 shows results for $\tilde{E}$ and $\tilde{\Gamma}$ plotted against $\alpha$. The case of the ring produced with a fixed orifice and a constant piston speed, $A$ and $B$, results in nondimensional energy values that are close to those of Gharib *et al.*,[5] however, the ring has clearly pinched-off in the case of $\sqrt{t_{\text{on}}/t_I}=4.0$. Figure 2(a) shows a significant amount of coherent vorticity trailing the lead vortex ring. This indicates that the formation number is affected by the apparatus. A possible explanation for this difference is that the vorticity thickness of the trailing jet is narrower for the orifice generator than tube generator. This would result in an earlier appearance of the Kelvin–Helmholtz instability and breakup of the trailing jet. The case of the accelerating piston, fixed diameter aperture, case $C$, shows a lower value of nondimensional energy with $\tilde{E} \sim 0.18$ and an associated increase in the Norbury parameter $\alpha \sim 0.85$, which also agrees well with the numerical simulations.[4,14] The case of the accelerating piston and opening aperture, case $D$, has a nondimensional energy that is similar to the fixed diameter, constant piston speed case with $\tilde{E} \sim 0.3$. This result can also be inferred from the vorticity field images shown in Fig. 2(b), which shows a vorticity distribution with a characteristic length scale that is of the order half the diameter of the ring. The most important result from this experiment is that it appears that case $E$, which consisted of closing the aperture while moving the piston with constant velocity, has been the most successful in terms of producing a ring of low nondimensional energy with $\tilde{E} \sim 0.17$ and an associated Norbury parameter of $\alpha \sim 0.95$. The vorticity plot in Fig. 2(c) shows a diffuse distribution of vorticity through the core which extends close to the axis of the vortex ring, which would be characteristic of a Hill's ring. In Fig. 2(c) the leading ring can be seen pinching-off from the trailing jet, indicating that the leading vortex is saturated and hence the pinch-off number $\sqrt{t_{\text{on}}/t_I}$ for this production characteristic is lower than that listed in Table I. The physical explanation for the successful production of a ring of low nondimensional energy is that, by closing the orifice

TABLE III. Ratios of measured ring properties to those predicted by the slug model with piston/aperture velocity characteristics described by programs *A*–*E*.

| | $\tilde{E}/\tilde{E}_{\text{slug}}$ | $\tilde{\Gamma}/\tilde{\Gamma}_{\text{slug}}$ | $\alpha/\alpha_{\text{slug}}$ | $U_t/U_{\text{exit}}$ | $\alpha_{\text{pinch}}$ |
|---|---|---|---|---|---|
| *A* | 0.5 | 1.3 | 5 | 0.63 | 0.35 |
| *B* | 1.0 | 0.8 | 1.3 | 0.74 | 0.35 |
| *C* | 0.6 | 1.2 | 1.6 | 0.47 | 0.74 |
| *D* | 0.45 | 1.2 | 3.5 | 0.56 | 0.53 |
| *E* | 0.5 | 1.2 | 2.4 | 1.0 | ⋯ |

while the ring is being formed we have continued to supply the ring with circulation, impulse, and kinetic energy via a jet of increasing velocity. While the speed of the ring has increased during generation, it has not been sufficient to escape from the feeding jet before the accumulation of invariants that result in a Hill's type ring. For fixed diameter orifices, the ring typically escapes from the feeding jet before a low nondimensional energy ring can be formed. It can be seen that the scatter in the data points shown in Figs. 1(a) and 1(b) is quite large. Based on an uncertainty level in the vorticity and stream function, measurement of ±5% results in calculated error of order ±18% in $\tilde{E}$ and ±10% in $\tilde{\Gamma}$. Further sources of error in the evaluation of the invariants and $\alpha$ are introduced via the selection of cutoff level of vorticity and the location of the $r=0$ axis. In order to evaluate this effect the cutoff level of vorticity was varied from 5% to 15% of the peak value. This was found to affect the results for the invariants and $\alpha$ of order ±10%. As a check, the circulation and kinetic energy invariants were calculated directly as contour and volume integrals of velocity, respectively. The results were found to agree within ±10% of the area integrals when using a vorticity level cutoff of 5%. Experimental scatter from repeated measurements can also serve as an indicator of measurement error. The error bars shown in Fig. 1(a) represent ±15%–25% in $\tilde{E}$ and in Fig. 1(b) the error bars are ±12% in $\tilde{\Gamma}$. These relatively conservative error bars capture the experimental data spread from multiple measurements fairly well. Despite the scatter the data points for $\tilde{E}$ and $\tilde{\Gamma}$ versus $\alpha$ are in general clustered around the Norbury curve.

In order to provide a rigorous description of the experimental trends we turn our attention to a model for pinch-off.[6] Based on our piston/aperture velocity characteristics it is possible to compute the nondimensional energy delivered to the flow, from the slug model, and hence correlate this result to an associated $\alpha_{\text{slug}}$, $\tilde{E}_{\text{slug}}$, and $\tilde{\Gamma}_{\text{slug}}$. The results for the predicted nondimensional energy, nondimensional circulation, and $\alpha$ from the slug model are shown in Table III compared with the measured values. From these results it is also clear that the slug model is not a highly accurate indicator of the invariants absorbed by the ring. The deficiency of the slug model in estimating circulation of a vortex ring has been noted previously and attributed to the following: (i) when the piston is initially started, the flow from the orifice resembles the potential flow solution of Pullin[16] and hence a higher rate of flux of circulation into the ring; (ii) ingestion of secondary vorticity formed on the walls of the generator during ring production;[1,17] (iii) that the slug model does not take into account the possibility of the formation of a Kelvin–Helmholtz instability in the trailing jet which has been suggested as being important in determining when the lead ring pinches-off from the trailing jet;[18] (iv) equating the impulse of the slug model to the impulse of the ring has been shown[2] to neglect the effects of an overpressure at the generation orifice and result in a significant underestimation of the impulse delivered to the flow prior to ring pinch-off.

Table III also shows the calculated pinch-off Norbury parameter $\alpha_{\text{pinch}}$ based on the technique proposed by Mohseni and Gharib,[6] using the velocity programs *A*-*B*. These results show an increased value of $\alpha$ for an accelerating piston, case *C*, compared to constant velocity piston case, case *B*. It also shows that for the opening aperture, accelerating piston, case *D*, there is no substantial difference to case *B*. These trends are seen in the experimental data. In the case of the closing aperture, constant piston speed the model does not display a crossing point, defined as $\partial E_{\text{slug}}/\partial I_{\text{slug}} = W_{\text{Norbury}}$, indicating that the slug model being a useful guide to vortex production should be used with caution when used as a predictive tool.


[1] N. Didden, "On the formation of vortex rings: Rolling-up and production of circulation," Z. Angew. Math. Phys. **30**, 101 (1979).
[2] P. S. Krueger and M. Gharib, "The significance of vortex ring formation to the impulse and thrust of a starting jet," Phys. Fluids **15**, 1271 (2003).
[3] D. Auerbach, "Stirring properties of vortex rings," Phys. Fluids A **3**, 1351 (1991).
[4] M. Rosenfeld, E. Rambod, and M. Gharib, "Circulation and formation number of laminar vortex rings," J. Fluid Mech. **376**, 297 (1998).
[5] M. Gharib, E. Rambod, and K. Shariff, "A universal time scale for vortex ring formation," J. Fluid Mech. **360**, 121 (1998).
[6] K. Mohseni and M. Gharib, "A model for universal time scale of vortex ring formation," Phys. Fluids **10**, 2436 (1998).
[7] J. Norbury, "A family of steady vortex rings," J. Fluid Mech. **57**, 417 (1973).
[8] L. E. Fraenkel, "Examples of steady vortex rings of small cross-section in an ideal fluid," J. Fluid Mech. **51**, 119 (1972).
[9] M. J. M. Hill, "On a spherical vortex," Philos. Trans. R. Soc. London, Ser. A **185**, 213 (1894).
[10] P. H. Roberts, "A Hamiltonian theory for weakly interacting vortices," Mathematika **19**, 168 (1972).
[11] J. J. Allen and B. Auvity, "Interaction of a vortex ring with a piston vortex," J. Fluid Mech. **465**, 353 (2002).
[12] G. Spedding and E. Rignot, "Performace analysis and application of grid interpolation techniques for fluid flows," Exp. Fluids **10**, 417 (1993).
[13] R. Verzicco, J. B. Flor, G. J. F. Van Heijst, and P. Orlandi, "Numerical and experimental analysis of the interaction between a dipole and a circular cylinder," Exp. Fluids **18**, 153 (1995).
[14] K. Mohseni, H. Ran, and T. Colonius, "Numerical experiments on vortex ring formation," J. Fluid Mech. **430**, 267 (2001).
[15] T. Naitoh, M. Kondoh, and J. J. Allen, "Formation of vortex rings using at variable diameter orifice," *Proceeding of the 2004 Meeting of Japan Society of Fluid Mechanics*, 2004.
[16] D. I. Pullin, "Vortex ring formation at tube and orifice openings," Phys. Fluids **22**, 401 (1979).
[17] D. Auerbach, "Experiments on the trajectory and circulation of the starting vortex," J. Fluid Mech. **183**, 185 (1987).
[18] W. Zhao, S. H. Frankel, and L. G. Mongeau, "Effects of trailing jet instability on vortex ring formation," Phys. Fluids **12**, 589 (2000).